Graphene Nanostructures Hot Paper

International Edition: DOI: 10.1002/anie.201602541
German Edition: DOI: 10.1002/ange.201602541

The Nanoparticle Size Effect in Graphene Cutting: A "Pac-Man" Mechanism

Zongyang Qiu, Li Song, Jin Zhao, Zhenyu Li, and Jinlong Yang*

Abstract: *Metal-nanoparticle-catalyzed cutting is a promising way to produce graphene nanostructures with smooth and well-aligned edges. Using a multiscale simulation approach, we unambiguously identified a "Pac-Man" cutting mechanism, characterized by the metal nanoparticle "biting off" edge carbon atoms through a synergetic effect of multiple metal atoms. By comparing the reaction rates at different types of edge sites, we found that etching of an entire edge carbon row could be triggered by a single zigzag-site etching event, which explains the puzzling linear dependence of the overall carbon-atom etching rate on the nanoparticle surface area observed experimentally. With incorporation of the nanoparticle size effect, the mechanisms revealed herein open a new avenue to improve controllability in graphene cutting.*

In many of the applications of two-dimensional (2D) atomic crystals,[1–3] a proper fabrication/manipulation method is a prerequisite. For example, graphene needs to be cut into nanoribbons for some electronics applications to utilize the resulting band gap[4,5] or edge states.[6] Graphene cutting can be carried out either in a strongly oxidative solution[7] or by applying highly energetic plasma.[8] However, to obtain smooth edges, a milder cutting environment is desirable. For this purpose, metal nanoparticles have been used as a catalyst to obtain well-aligned graphene channeling.[9–20] Impressively, almost 100% zigzag edges have been obtained by using Ni-nanoparticle-catalyzed cutting of monolayer graphene in a H_2/Ar atmosphere.[14]

To better control the cutting process, the underlying atomic mechanisms should be understood.[21–24] Currently, the unzipping mechanism[7,25–27] is the dominant graphene-cutting mechanism reported in the literature, where C–C bonds in graphene are broken by single cutting atoms and the nanoparticle size is thus irrelevant. However, significant nanoparticle size effects on both the cutting behavior and the resulting graphene edge morphology have been observed experimentally.[10,13,14] An interesting example is the linear dependence of the overall etching rate on the square of the nanoparticle radius (R^2),[28,29] which seems to indicate that graphene cutting is controlled by a reaction on the nanoparticle surface. Hydrogen decomposition and carbon hydrogenation are the two possible surface reactions in graphene cutting. However, the absence of a hydrogen pressure effect[29] excludes the possibility of hydrogen decomposition as the rate-limiting step. At the same time, if carbon hydrogenation was the rate-limiting step, dissolved C atoms would either form carbide or precipitate out after cutting, which is not observed experimentally.[13,20] Therefore, a consistent cutting mechanism remains to be fully elucidated.

In this Communication, by combining density functional theory (DFT), reactive molecular dynamics (MD), metadynamics,[30] and kinetic Monte Carlo (kMC) simulations, we identify a "Pac-Man" mechanism for Ni-nanoparticle-catalyzed cutting, with C–C bond breaking at the graphene–metal interface as the rate-limiting step. A zigzag-triggered edge-etching behavior is found to be the reason for the experimentally observed R^2 dependence of the overall etching rate.

First, an MD simulation is performed with a Ni nanoparticle close to graphene edges and some H_2 molecules initially in the gas phase, to obtain the overall picture of graphene cutting (Figure 1 a). Hydrogen passivation of graphene edges and their dissociative adsorption on the Ni surface are

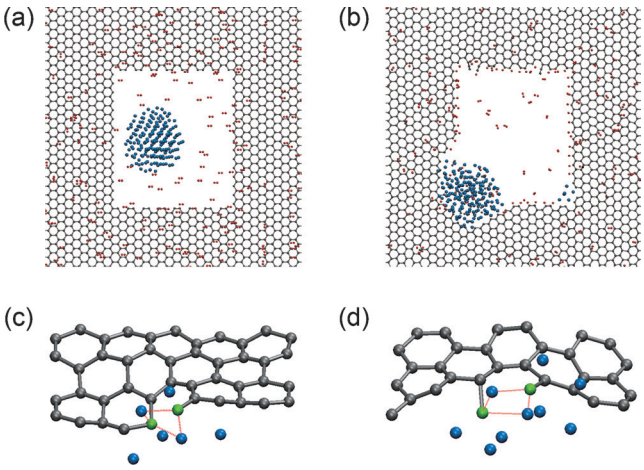

Figure 1. a) Initial and b) final configurations of a 7 ns MD simulated trajectory at 2000 K. C = gray, Ni = blue, H = red. Expanded portions showing C–C bond breaking at c) zigzag and d) armchair edges. For clarity, in (c) and (d) all H_2 molecules and Ni atoms more than 3.0 Å from the two corresponding carbon atoms (shown in green) are not shown. C–Ni–C bridges are highlighted by red dashed lines.

[*] Z. Qiu, Prof. J. Zhao, Prof. Z. Li, Prof. J. Yang
Hefei National Laboratory for Physical Sciences at the Microscale
CAS Centre for Excellence and Synergetic Innovation Center of Quantum Information & Quantum Physics
University of Science and Technology of China
Hefei, Anhui 230026 (China)
E-mail: zyli@ustc.edu.cn
Prof. L. Song
National Synchrotron Radiation Laboratory
University of Science and Technology of China
Hefei, Anhui 230026 (China)
Supporting information and the ORCID identification number(s) for the author(s) of this article can be found under http://dx.doi.org/10.1002/anie.201602541.

observed at an early stage of the MD simulation. After 500 ps, edge C–C bond breaking at the graphene–metal interface starts, generating etched C atoms which diffuse into the nanoparticle. These dissolved C atoms finally react with decomposed H atoms on the nanoparticle surface to form hydrocarbon species, such as C_2H, CH, and CH_4. Such a carbon dissolution mechanism[10,28] is consistent with the fact that hydrogen adsorbs stronger on the Ni surface than at the graphene edges.[31]

C–C bond breaking is catalyzed by Ni atoms without any involvement of H atoms. The Ni–C interaction can weaken and finally break an edge C–C bond by inserting two bridging Ni atoms (Figure 1 c,d). Then, the resulting dangling C atoms are surrounded by adjacent Ni atoms including those two bridging atoms, typically with a distortion of the dangling bonds out of the graphene plane. Finally, the enclosed C atoms are taken up by the nanoparticle, similar to a Pac-Man eating dots.

Sequential C atom etching leads to a graphene channeling, or cutting, by the Ni nanoparticle. The main driving force of such a cutting is the strong Ni–C interaction,[10,13,21] as demonstrated by the close contact between the Ni nanoparticle and graphene edges. As a requirement of the cutting, the shape of the nanoparticle does not change much during its movement, indicating a high cohesive energy and/or a strong surface tension. The availability of H atoms to passivate newly formed graphene edges also facilitates the cutting. Newly formed graphene edges are mainly zigzag in character (Figure 1 b) because C etching, as a synergic effect of multiple Ni atoms, preferentially proceeds at the more open and flexible armchair edge.[32]

Metadynamics simulations are used to obtain the free energy surface in a space defined by a few collective variables (CVs). For zigzag edge etching, C_1C_2 and C_2C_3 bond lengths (Figure 2 a) are used to construct the free energy surface, which has four minima corresponding to the configurations with a pristine edge, a broken C_1C_2 bond, a broken C_2C_3 bond, and with C_2 etched away, respectively (see Figure S1 in the Supporting Information). The free energy barrier for the first C–C bond breakage (either C_1C_2 or C_2C_3) is 1.73 eV.

For armchair edge etching, the coordination numbers of C_2 and C_3 (CN_2 and CN_3) are used as the CVs. The obtained free energy surface (Figure 2 e) has minima at the different (CN_2, CN_3) configurations shown in Figure 2 d. In the most favorable pathway, the C_2C_3 bond breaks first with a 1.11 eV free energy barrier (much lower than that in the zigzag case), followed by the simultaneous breaking of the two resulting dangling bonds with a barrier of 0.97 eV.

Based on the physical picture obtained with the above-mentioned information, high-level DFT calculations could be performed by constructing a minimal but still physical model (typically with 4–6 Ni atoms) for the Ni nanoparticle. As shown in Figure 3, zigzag-edge bond breaking has a much higher energy barrier (1.45 eV) compared to that of armchair bonds (0.50 eV). At the armchair edge, after the C_2C_3 bond breaking, the resulting dangling bonds can be broken by overcoming an energy barrier of 0.73 eV.

To compare with the unzipping mechanism,[7,25–27] we also construct models with only one Ni atom included. At the

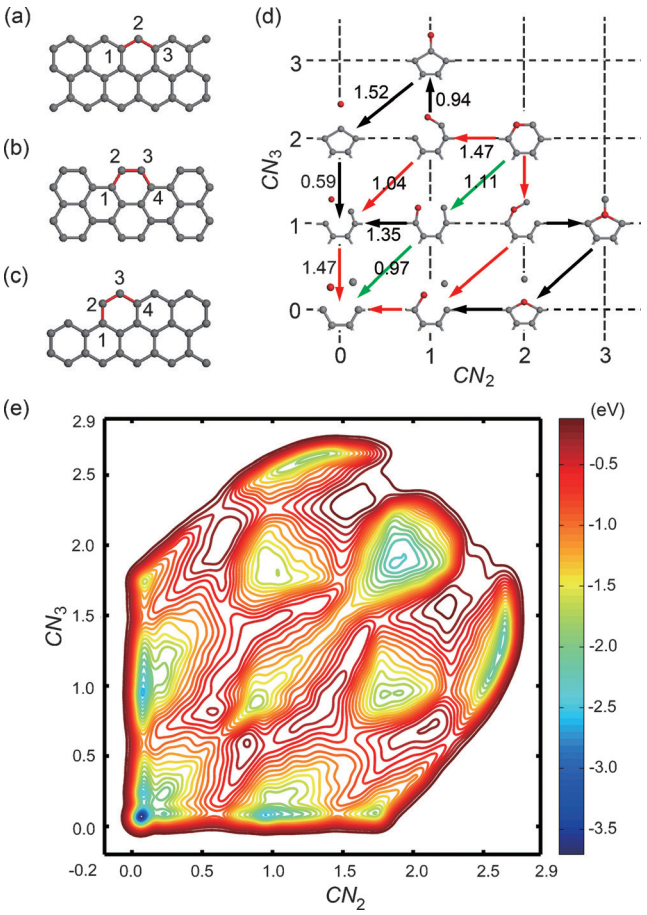

Figure 2. Structures of a) zigzag, b) armchair, and c) kink sites. Relevant edge atoms are numbered to label different C–C bonds. d) Different armchair edge configurations identified by CN_2 and CN_3. The free energy barrier associated with each configuration change is marked in eV. e) Free energy surface obtained from a metadynamics simulation at 1200 K.

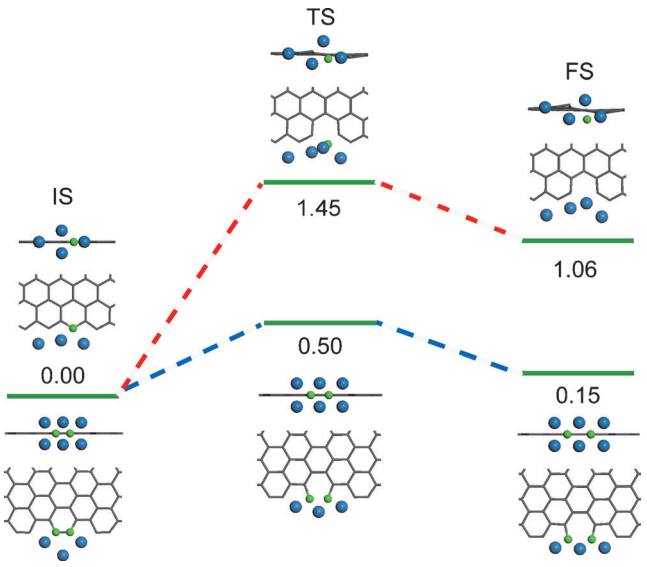

Figure 3. Minimum energy paths of Ni-catalyzed C–C bond breaking at zigzag and armchair edges from DFT calculations. IS = initial state; TS = transition state; FS = final state. Values are given in eV.

zigzag edge, one Ni atom requires 1.93 eV to break the edge C–C bond. For the armchair edge, 2.84 and 1.82 eV are required for one Ni atom to break the C_2C_3 and C_1C_2 bonds, respectively. Such high barriers indicate that the unzipping mechanism is unfavorable compared to the Pac-Man mechanism described herein. It should also be remarked that if an ideal surface is used to model the Ni nanoparticle, the C–C bond-breaking barrier is even higher.[33]

Both ab initio and empirical calculations predict a relatively high C–C bond-breaking barrier (1.5–1.7 eV at the zigzag edge) compared to other competing processes. For example, the C diffusion barrier in the Ni nanoparticle is only 0.23 eV at 1200 K (Figure S8). At the same time, there is also a consistent barrier difference between zigzag and armchair site etching, which can lead to a C–C bond-breaking rate difference of several orders of magnitude at 1200 K. Therefore, once a zigzag carbon atom is etched away, the formed kink sites, which are essentially a very short armchair fragment (Figure 2c), can be rapidly etched off, which finally leads to the disappearance of the corresponding whole zigzag edge row.

Such a triggering behavior naturally leads to a new explanation of the R^2-dependent kinetics observed experimentally. To confirm this, kMC simulations were carried out. The overall etching rate k, defined as the number of etched C atoms per unit time, is indeed proportional to the R^2 value (Figure 4a) in our simulations, since the time (t) spent for a fixed nanoparticle moving distance is inversely proportional to the R value (Figure 4b). In fact, the larger the nanoparticle, the longer the graphene–metal interface and the more available zigzag carbon atoms, which then leads to a shorter waiting time before triggering of a zigzag etching event. When looking at the types of atoms being etched, we consistently find that most of the C atoms are etched at kink sites (Figure 4c) while the etching time is mainly consumed by those rare zigzag-site etching events (Figure 4d).

The triggering behavior also provides us new insights into other experimental observations. For example, it is consistent with the previously reported discrete dynamics of nanoparticle channeling.[15] The behavior also explains the trend in multilayer graphene cutting where shallow channels are typically longer than deeper channels.[10] Etching of different graphene layers is expected to be independent. Therefore, the nanoparticle movement is determined by the layer triggered last and thus becomes slower for thicker graphene.

In summary, we have systematically studied the Ni nanoparticle etching behavior at different graphene edge sites and identified a Pac-Man-like mechanism characterized by a synergic effect of multiple Ni atoms. In this mechanism, forming close contact between graphene edges and the Ni nanoparticle is essential. Therefore, it is much easier to etch the more open and flexible armchair edge sites compared to zigzag edge sites. This result in turn has enabled us to explain why experimentally the observed cutting rate is proportional to the nanoparticle surface area, based on a rate-limiting step at the graphene–metal interface. By combining these findings, the whole atomic picture of graphene cutting has been revealed, which is not only key to gain more precise control of graphene cutting but is also expected to stimulate substantial future studies of the processing and fabrication of 2D materials.

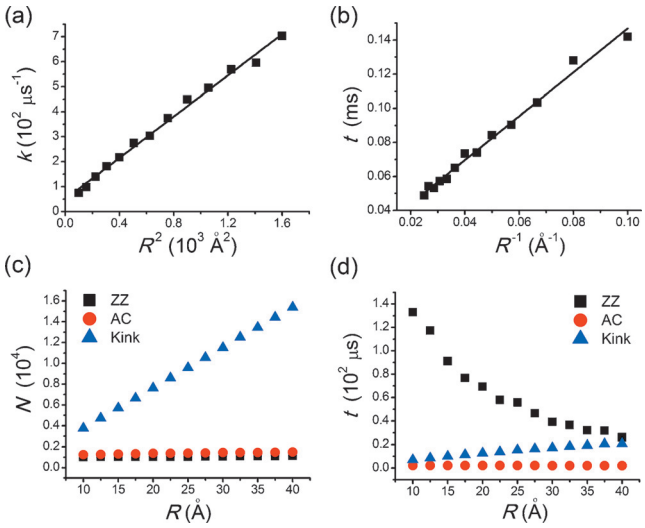

Figure 4. Plots showing the variation of the a) overall etching rate (k) versus R^2, b) the etching time (t) for a 1065 Å channel length versus R^{-1}, c) the numbers (N) of etched zigzag (ZZ), armchair (AC), and kink-site C atoms versus R, and d) their consumed etching time versus R.

Acknowledgements

This work was partially supported by the NSFC (21421063 and 21573201), the MOST (2014CB932700), the CAS (XDB01020300), the CUSF, the NSFC-Guangdong Joint Fund, and by USTC-SCC, SCCAS, Tianjin, and Shanghai Supercomputer Centers.

Keywords: density functional calculations · graphene · multiscale simulations · nanoparticles · nickel

How to cite: *Angew. Chem. Int. Ed.* **2016**, *55*, 9918–9921
Angew. Chem. **2016**, *128*, 10072–10075

[1] F. Schwierz, *Nature* **2011**, *472*, 41.
[2] A. N. Abbas, G. Liu, A. Narita, M. Orosco, X. Feng, K. Mullen, C. Zhou, *J. Am. Chem. Soc.* **2014**, *136*, 7555.
[3] K. Celebi, J. Buchheim, R. M. Wyss, A. Droudian, P. Gasser, I. Shorubalko, J. I. Kye, C. Lee, H. G. Park, *Science* **2014**, *344*, 289.
[4] Y. Son, M. L. Cohen, S. G. Louie, *Phys. Rev. Lett.* **2006**, *97*, 216803.
[5] M. Y. Han, B. Özyilmaz, Y. Zhang, P. Kim, *Phys. Rev. Lett.* **2007**, *98*, 206805.
[6] Y. Son, M. L. Cohen, S. G. Louie, *Nature* **2006**, *444*, 347.
[7] J. L. Li, K. N. Kudin, M. J. McAllister, R. K. Prudhomme, I. A. Aksay, R. Car, *Phys. Rev. Lett.* **2006**, *96*, 176101.
[8] L. Xie, L. Jiao, H. Dai, *J. Am. Chem. Soc.* **2010**, *132*, 14751.
[9] S. Konishi, W. Sugimoto, Y. Murakami, Y. Takasu, *Carbon* **2006**, *44*, 2338.
[10] L. Ci, Z. Xu, L. Wang, W. Gao, F. Ding, K. F. Kelly, B. I. Yakobson, P. M. Ajayan, *Nano Res.* **2008**, *1*, 116.

[11] S. S. Datta, D. R. Strachan, S. M. Khamis, A. C. Johnson, *Nano Lett.* **2008**, *8*, 1912.
[12] N. Severin, S. Kirstein, I. Sokolov, J. Rabe, *Nano Lett.* **2009**, *9*, 457.
[13] F. Schäffel, J. H. Warner, A. Bachmatiuk, B. Rellinghaus, B. Büchner, L. Schultz, M. H. Rümmeli, *Nano Res.* **2009**, *2*, 695.
[14] L. C. Campos, V. R. Manfrinato, J. D. Sanchez-Yamagishi, J. Kong, P. Jarillo-Herrero, *Nano Lett.* **2009**, *9*, 2600.
[15] T. J. Booth, F. Pizzocchero, H. Andersen, T. W. Hansen, J. B. Wagner, J. R. Jinschek, R. E. Dunin-Borkowski, O. Hansen, P. Bøggild, *Nano Lett.* **2011**, *11*, 2689.
[16] M. Lukas, V. Meded, A. Vijayaraghavan, L. Song, P. M. Ajayan, K. Fink, W. Wenzel, R. Krupke, *Nat. Commun.* **2013**, *4*, 1379.
[17] J. Wei, Z. Xu, H. Wang, X. Tian, S. Yang, L. Wang, W. Wang, X. Bai, *Nanotechnology* **2014**, *25*, 465709.
[18] G. Melinte, I. Florea, S. Moldovan, I. Janowska, W. Baaziz, R. Arenal, A. Wisnet, C. Scheu, S. Bégin-Colin, D. Bégin, et al., *Nat. Commun.* **2014**, *5*, 4109.
[19] F. Pizzocchero, M. Vanin, J. Kling, T. W. Hansen, K. W. Jacobsen, P. Bøggild, T. J. Booth, *J. Phys. Chem. C* **2014**, *118*, 4296.
[20] D. Díaz-Fernández, J. Méndez, A. del Campo, R. Mossanek, M. Abbate, M. Rodríguez, G. Domínguez-Cañnizares, O. Bomatí-Miguel, A. Gutiérrez, L. Soriano, *Carbon* **2015**, *85*, 89.
[21] S. S. Datta, *J. Appl. Phys.* **2010**, *108*, 024307.
[22] L. Ma, J. Wang, F. Ding, *Angew. Chem. Int. Ed.* **2012**, *51*, 1161; *Angew. Chem.* **2012**, *124*, 1187.
[23] T. Zoberbier, T. W. Chamberlain, J. Biskupek, J. Biskupek, N. Kuganathan, S. Eyhusen, E. Bichoutskaia, U. Kaiser, A. N. Khlobystov, *J. Am. Chem. Soc.* **2012**, *134*, 3073.
[24] L. Ma, J. Wang, F. Ding, *ChemPhysChem* **2013**, *14*, 47.
[25] J. Wang, L. Ma, Q. Yuan, L. Zhu, F. Ding, *Angew. Chem. Int. Ed.* **2011**, *50*, 8041; *Angew. Chem.* **2011**, *123*, 8191.
[26] Z. Li, W. Zhang, Y. Luo, J. Yang, J. G. Hou, *J. Am. Chem. Soc.* **2009**, *131*, 6320.
[27] Q. Chen, L. Ma, J. Wang, *WIREs Comput. Mol. Sci.* **2016**, 6, 243.
[28] C. Keep, S. Terry, M. Wells, *J. Catal.* **1980**, *66*, 451.
[29] P. J. Goethel, R. T. Yang, *J. Catal.* **1987**, *108*, 356.
[30] A. Laio, M. Parrinello, *Proc. Natl. Acad. Sci. USA* **2002**, *99*, 12562.
[31] G. J. Soldano, P. Quaino, E. Santos, W. Schmickler, *J. Phys. Chem. C* **2013**, *117*, 19239.
[32] J. Kotakoski, D. Santos-Cottin, A. V. Krasheninnikov, *ACS Nano* **2012**, *6*, 671.
[33] L. Ma, J. Wang, J. Yip, F. Ding, *J. Phys. Chem. Lett.* **2014**, *5*, 1192.

Received: March 12, 2016
Revised: April 12, 2016
Published online: May 24, 2016

